Impedance of an induction coil at the opening of a borehole in a conductor

Theodoros P. Theodoulidis and John R. Bowler

Citation: J. Appl. Phys. **103**, 024905 (2008); doi: 10.1063/1.2827459
View online: http://dx.doi.org/10.1063/1.2827459
View Table of Contents: http://jap.aip.org/resource/1/JAPIAU/v103/i2
Published by the American Institute of Physics.

Impedance of an induction coil at the opening of a borehole in a conductor

Theodoros P. Theodoulidis
Department of Engineering and Management of Energy Resources, West Macedonia University, 50100 Kozani, Greece

John R. Bowler[a)]
Center for Nondestructive Evaluation, Iowa State University, Iowa 50011, USA

(Received 4 October 2007; accepted 29 October 2007; published online 17 January 2008)

The electromagnetic field of a cylindrical eddy current probe coil near the open end of a borehole in a conductor has been calculated analytically accounting for edge effects. Calculations of the coil impedance as a function of position and excitation frequency have been made allowing theoretical results to be compared with experimental measurements. Comparisons have been carried out for special cases in which a cylindrical coil has its axis either perpendicular or parallel to the axis of the hole. In the approach used, the field is expressed in terms of transverse electric and transverse magnetic potentials defined with respect to the axis of the hole. The domain of the problem is truncated in the axial direction in order to express the solution in the form of eigenfunction expansions. The truncation modifies the original unbounded domain problem, but the additional boundaries can be made as remote from the coil as desired so that they have a negligible effect on numerical estimates of the coil field. The truncated region approach has proved to be accurate and computationally efficient but more significantly, it allows new solutions to be found for problems that are otherwise analytically intractable. The results model eddy current inspections of boreholes including edge effects at the opening of the hole. © *2008 American Institute of Physics*.
[DOI: 10.1063/1.2827459]

I. INTRODUCTION

Closed form solutions for the quasistatic electromagnetic field in cylindrical systems[1] have been used extensively for studying eddy current coil interactions with infinite holes, pipes, and rods. Recently, a new class of analytical solutions has become accessible by truncation of an otherwise infinite domain problem in one or more coordinate directions, allowing modal quasistatic solutions to be found for a penetrable conductive wedge[2] and tube end effects.[3] Here, the approach is used to determine the field and impedance of a coil at the opening of a semi-infinite borehole (Fig. 1). With minor modifications, the calculations can be extended to deal with a coil in a borehole through a plate.

The edge of a borehole is a critical region where cracks can initiate in components under stress, and although we do not deal here with the fields due to cracks, the approach given can be used to derive a Green's kernel in analytical form for a singular source near the borehole opening and, thereby, provide a means for performing crack calculations via integral methods using a dedicated kernel for this important structure.

In applying the truncated region eigenfunction expansion method, an approximate analytic solution is sought in the form of an eigenfunction expansion. In a cylindrical system, the problem domain can be truncated in the radial direction[4] or the axial direction,[5] depending on the nature of the problem. This can be done without introducing significant errors, provided that the field at the truncation boundaries would otherwise be small. In the case of an axial truncation, the procedure means that the axial dependence can be expressed in the form of Fourier series. By approximating the infinite series with a finite number of terms, the boundary value problem reduces to one of finding a finite number of expansion coefficients. The expansion coefficients for different regions (Fig. 2) are used to form column vectors. Matrix relationships between the vectors are derived using continuity conditions on the field at the radial interfaces. One coefficient vector is used to represent a predefined source coil field and the remaining coefficient vectors are expressed in terms of the source vector by a process of elimination. In this way, a solution is found.

The procedure is computationally efficient and errors are easily controlled by simply adjusting the location of the truncation boundaries or by modifying the number of terms in the Fourier series. The analytical advantage is that approximate solutions can be derived for new configurations by adapting traditional canonical structures. An example is the canonical problem of finding the electromagnetic field in an infinite tube due to an internal coaxial coil. This problem can be modified in the truncated region to get a solution for the

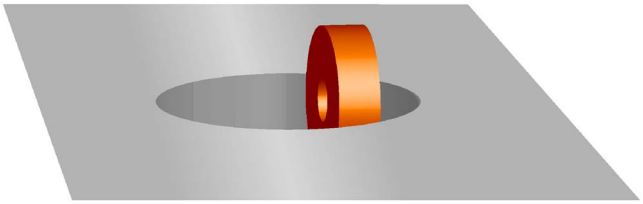

FIG. 1. (Color online) Coil at the opening of a borehole, the axis of the coil being perpendicular to the axis of the hole.

[a)]Electronic mail: jbowler@iastate.edu.

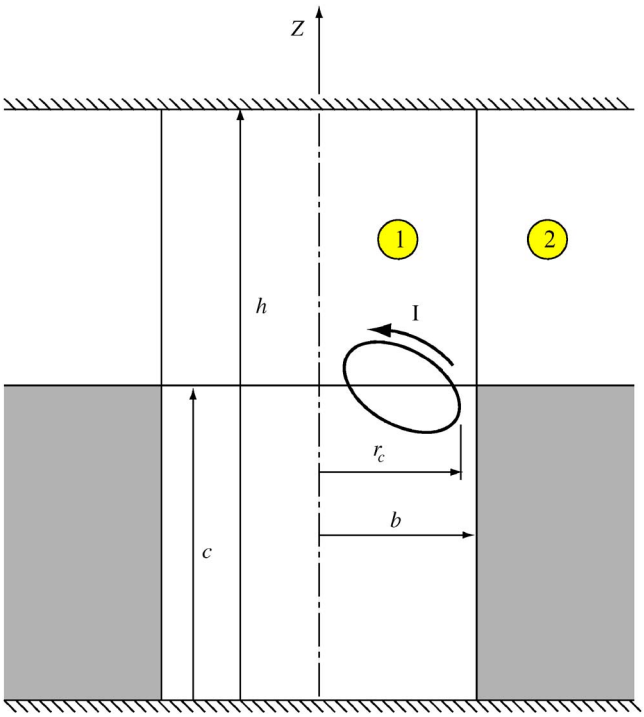

FIG. 2. (Color online) An arbitrarily shaped coil in the region of the mouth of a borehole. The domain of the electromagnetic field problem is truncated at the planes $z=0$ and $z=h$.

tube end effect.[3] Here, we examine the calculation of the field of an arbitrary coil carrying a current varying as the real part of $Ie^{j\omega t}$ in a cylindrical hole within a domain which is finite in the axial direction (Fig. 2). We seek the electromagnetic field at the edge of the hole and the change in coil impedance as its vertical position is varied by relating these quantities to the source coil coefficients evaluated for a homogeneous region. Expressions for the source coefficients are derived for a coil whose axis is perpendicular to that of the hole, referred to as a rotary coil, and also for an offset bobbin coil whose axis is parallel to and displaced from that of the hole.

II. FORMULATION

The initially infinite domain problem is truncated in the axial direction to limit the axial coordinate range to $0 \leqslant z \leqslant h$ (Fig. 2). By locating the coil sufficiently far from the upper and lower boundaries, the truncation error can be set at a tolerable level. The quasistatic magnetic flux density is here expressed in terms of scalar potentials,

$$\mathbf{B} = \nabla \times \nabla \times [\hat{z} W_a] + k^2 \nabla \times [\hat{z} W_b], \tag{1}$$

where $k^2 = j\omega\mu_0\sigma$. Both the transverse electric (TE) W_a and transverse magnetic (TM) potentials W_b satisfy the Helmholtz equation,

$$(\nabla^2 - k^2) W = 0. \tag{2}$$

The Fourier series representation with respect to the azimuthal angle is written as

$$W(\rho, \varphi, z) = \sum_{m=-\infty}^{\infty} \tilde{W}_m(\rho, z) e^{jm\varphi}. \tag{3}$$

Then, the solution $\tilde{W}_m(\rho, z)$ for the conductive region, for example, has terms of the form

$$(A_0 r^m + B_0 r^{-m})(C + Dz) + [A(u)\sin(uz) + B(u)\cos(uz)] \times [C(u) I_m(pr) + D(u) K_m(pr)],$$

where $I_m(x)$ and $K_m(x)$ are associated Bessel functions and $p = \sqrt{u^2 + k^2}$. For nonconductive regions, we have a similar expression with $k^2 = 0$. Because of the truncation in the axial direction, the z dependence of the field is expressed as a Fourier series with u having discrete values. Continuity conditions are then used to determine the solution coefficients.

For reference, the components of the magnetic field are stated here in a form that is convenient for applying interface conditions,

$$\tilde{B}_\rho = \frac{\partial \psi_m}{\partial \rho} + Jm \frac{1}{\rho} \phi_m, \tag{4}$$

$$\tilde{B}_\varphi = Jm \frac{1}{\rho} \psi_m - \frac{\partial \phi_m}{\partial \rho}, \tag{5}$$

$$\tilde{B}_z = \frac{\partial \psi_m}{\partial z} - k^2 \tilde{W}_{am}, \tag{6}$$

where we use the magnetic scalar potential ψ defined such that $\psi = \partial W_a / \partial z$ and write

$$\psi_m = \frac{\partial \tilde{W}_{am}}{\partial z}, \quad \phi_m = k^2 \tilde{W}_{bm} \tag{7}$$

to represent the TE and TM modes, respectively. In the nonconductive region $\mathbf{B} = \nabla \psi$.

A. Formal solution

The potential and expansion coefficients representing the source field in the absence of induced current are denoted by the superscript (0). Similarly, the superscript (1) is associated with quantities representing the field in region 1 due to induced current (Fig. 2). In this scheme, the TE potential in region 1 is the sum of contributions from the source and from induced currents, written as $\psi_m^{(0)} + \psi_m^{(1)}$. For the whole of the region $\rho > b$ $(0 \leqslant z \leqslant h)$, the quantities representing the TE potential are denoted by the superscript (2).

In constructing the formal solution, we use series expressions for the transformed TE and TM potentials that are solutions of the Helmholtz or Laplace equations depending on whether the region considered is conductive or not, respectively. At the formal stage of the development, the continuity of the field in the plane $z=c$ (Fig. 2) is also considered. The basic requirements at the horizontal planes are satisfied first before imposing continuity of the field at the radial interface between region 1 and region 2, as described in Sec. III.

On the truncation boundaries at $z=0$ and $z=h$, we impose the condition that the tangential electric field is zero. It follows that the normal component of the magnetic flux den-

sity on these boundaries is also zero. Setting $\mathbf{E}_t=0$ at $z=0$ effectively imposes a parity condition with respect to the z dependence of the solution since the tangential electric field due to a coil can be nulled by the field of an image probe placed below the $z=0$ plane carrying a current in the opposite sense to that of the original source coil. We define the parity in terms of the source-image relationship which in this case has odd parity. One can generate both odd and even parity solutions, then sum them to eliminate the effect of the image coil and halve the solution to represent the field due to a coil in a finite thickness or a thin plate. However, we do not give the details of this calculation but instead use the odd parity solution for a calculation of the coil field at the mouth of a semi-infinite hole approximated as having a large but finite depth c. The even parity solution could also be used for this task since the field in the presence of a semi-infinite hole is approximated in a finite region whose boundaries are remote from the entrance to the hole and the coil. Hence, we need only choose a boundary condition at $z=0$ and $z=h$ that approximates the small field that would otherwise exist at these planes if the domain was not truncated.

Expressions for the transformed TE and TM potentials that satisfy the truncation boundary conditions at $z=0$ and $z=h$ are stated as follows. Starting with the TE source potential at a point outside the outer limit of the probe coil $(\rho>r_c)$,

$$\psi_m^{(0)}(\rho,z)=\left(\frac{\rho}{b}\right)^{-m}C_{m0}^{(0)}+\sum_{i=1}^{\infty}\cos u_i z\left[\frac{K_m(u_i\rho)}{K_m(u_i b)}\right]C_{mi}^{(0)}. \quad (8)$$

For the part of region 1 in which $b>\rho>r_c$, the potential due to induced current is

$$\psi_m^{(1)}(\rho,z)=\left(\frac{\rho}{b}\right)^{m}C_{m0}^{(1)}+\sum_{i=1}^{\infty}\cos u_i z\left[\frac{I_m(u_i\rho)}{I_m(u_i b)}\right]C_{mi}^{(1)}. \quad (9)$$

The cosine dependence ensures that $\partial\psi_m/\partial z=0$ and, hence, $\tilde{B}_z=0$ at $z=0$. Putting $u_i=i\pi/h$ ensures that $\partial\psi_m/\partial z=0$ at $z=h$. Factors containing b are included in these expressions in anticipation of being able to simplify expressions for the field at the $\rho=b$ boundary.

For region 2, the TE potential has the form

$$\psi_m^{(2)}(\rho,z)=\begin{cases}\displaystyle\sum_{i=1}^{\infty}\cos q_i z\left[\frac{K_m(p_i\rho)}{K_m(p_i b)}\right]C_{mi}^{(2)}, & 0\leqslant z\leqslant c,\\ \displaystyle\left(\frac{\rho}{b}\right)^{-m}C_{m0}^{(2)}+\sum_{i=1}^{\infty}\cos[p_i(h-z)]\left[\frac{K_m(p_i\rho)}{K_m(p_i b)}\right]\alpha_i C_{mi}^{(2)}, & c\leqslant z\leqslant h,\end{cases} \quad (10)$$

where $p_i^2=q_i^2+k^2$. The q_i eigenvalues are found using the continuity of H_ϕ and H_ρ at $z=c$ $(\rho\geqslant b)$ following a procedure described in Ref. 2. This gives

$$\alpha_i=\frac{\cos q_i c}{\cos[p_i(h-c)]}=-\frac{p_i\sin q_i c}{q_i\sin[p_i(h-c)]}. \quad (11)$$

Hence, the eigenvalues are the roots of the complex transcendental equation

$$\sqrt{q_i+k^2}\tan q_i c+q_i\tan[p_i(h-c)]=0. \quad (12)$$

It is only necessary to compute these roots once for a given ratio of c/h since they are independent of m. Typically, less than 100 roots are used depending on the number of terms chosen for the series representation. A suitable root finding routine can be used for the purpose.

The TM potential for the conductive region is expressed as

$$\phi_m(\rho,z)=\cosh kz\left(\frac{\rho}{b}\right)^{-m}D_{m0}+\sum_{i=1}^{\infty}\cos r_i z\left[\frac{K_m(s_i\rho)}{K_m(s_i b)}\right]D_{mi},$$
$$0\leqslant z\leqslant c. \quad (13)$$

Putting $r_i=(i-\frac{1}{2})\pi/c$ ensures that the normal component of the current at the surface of the conductor, approached from within it, is zero. Letting $s_i^2=r_i^2+k^2$ guarantees that Eq. (2) is satisfied by all terms in the summation. By taking the curl of Eq. (1) to find the electric field and using Eq. (2), it can be seen that the z component of the electric field is zero if

$$\frac{\partial^2\phi_m}{\partial z^2}-k^2\phi_m=0. \quad (14)$$

The leading term in the series, which is actually a transverse electric and magnetic mode, conforms to this requirement.

A relationship between $C_{m0}^{(2)}$ and D_{m0} is found from the continuity of H_ϕ at $z=c(\rho\geqslant b)$, which gives

$$C_{m0}^{(2)}=-J\cosh(kc)D_{m0}. \quad (15)$$

This completes the formal stage of the development. Next, we impose the appropriate continuity conditions that govern the field at $\rho=b$.

III. CONTINUITY AT THE RADIAL INTERFACE

The continuities of the tangential magnetic field and the normal component of the magnetic flux density are applied in the weak sense for the interface $\rho=b$. Matching firstly H_φ integrated between $z=0$ and $z=h$, we find that

$$jm[C_{m0}^{(0)} + C_{m0}^{(1)}] = \frac{m}{\lambda} D_{m0} - \frac{b}{h} \sum_{i=1}^{\infty} \frac{s_i}{r_i} \sin(r_i c) \frac{K_m'(s_i b)}{K_m(s_i b)} D_{mi}, \tag{16}$$

whereas matching B_ρ across the $\rho = b$ interface by integrating over the same range shows that

$$J[C_{m0}^{(0)} - C_{m0}^{(1)}] = \frac{1}{\lambda} D_{m0} + \frac{1}{h} \sum_{i=1}^{\infty} \frac{1}{r_i} \sin(r_i c) \frac{K_m'(s_i b)}{K_m(s_i b)} D_{mi}, \tag{17}$$

where

$$\lambda = \frac{hk}{\sinh kc + k(h-c)\cosh kc}. \tag{18}$$

These relationships combine with the help of expressions for the derivative of the associated Bessel function[6] to give

$$C_{m0}^{(1)} = -\frac{j}{m} \mathbf{R}_{m-1}^T \mathbf{D}_m \tag{19}$$

and

$$D_{m0} = \lambda \left[J C_{m0}^{(0)} - \frac{1}{m} \mathbf{R}_{m+1}^T \mathbf{D}_m \right], \tag{20}$$

where we have used the superscript T to denote the transpose of a column vector and have formed the scalar product of a column vector whose components are

$$R_{m\pm1,i} = \frac{b}{2h} \frac{s_i}{r_i} (-1)^{i+1} \frac{K_{m\pm1}(s_i b)}{K_m(s_i b)}, \tag{21}$$

with a vector $\mathbf{D}_m$ representing the expansion coefficients for the TM potential.

Equations (15), (19), and (20) allow us to eliminate unknown zero order coefficients. Then, matrix equations for the remaining three sets of unknown coefficients are found by matching at the $\rho = b$ boundary $H_z \sin u_j z$, $H_\varphi \cos u_j z$, and $B_\rho \cos u_j z$, integrated between 0 and h. Applying trigonometric function orthogonality relations,

$$\int_0^h \sin u_j z \sin u_i z dz = \frac{h}{2} \delta_{ij} \quad \int_0^h \cos u_j z \cos u_i z dz = \frac{h}{2} \delta_{ij}, \tag{22}$$

we obtain the following system:

$$\mathbf{u}\left[\mathbf{C}_m^{(0)} + \mathbf{C}_m^{(1)}\right] = \mathbf{M}_s \mathbf{p} \mathbf{C}_m^{(2)}, \tag{23}$$

$$Jm[\mathbf{C}_m^{(0)} + \mathbf{C}_m^{(1)}] = Jm\mathbf{M}_c \mathbf{C}_m^{(2)} - [b\mathbf{M}_r \mathbf{s} M_m(\mathbf{s}b) + \lambda \mathbf{L} \mathbf{R}_{\mathbf{m}+1}^T] \mathbf{D}_m + Jm\lambda \mathbf{L} C_{m0}^{(0)}, \tag{24}$$

$$b\mathbf{u}[M_m(\mathbf{u}b)\mathbf{C}_m^{(0)} + \Lambda_m(\mathbf{u}b)\mathbf{C}_m^{(1)}] = b\mathbf{M}_c \mathbf{p} M_m(\mathbf{p}b)\mathbf{C}_m^{(2)} + J[m\mathbf{M}_r - \lambda \mathbf{L} \mathbf{R}_{m+1}^T] \mathbf{D}_m - m\lambda \mathbf{L} C_{m0}^{(0)}. \tag{25}$$

Here, $\mathbf{C}_m^{(0)}$, $\mathbf{C}_m^{(0)}$, and $\mathbf{C}_m^{(2)}$, are column vectors of expansion coefficients, whereas $\mathbf{u}$, $\mathbf{p}$, $\mathbf{s}$, $M_m(\mathbf{u}b)$, and $\Lambda_m(\mathbf{u}b)$ are diagonal matrices and we have defined

$$M_m(z) = \frac{K_m'(z)}{K_m(z)}, \quad \Lambda_m(z) = \frac{I_m'(z)}{I_m(z)}. \tag{26}$$

Other matrices in Eqs. (23)–(25) have elements defined by

$$M_s[i,j] = \frac{2}{h} \left[\frac{p_j}{q_j} \int_0^c \sin u_i z \sin q_j z dz - \alpha_j \int_c^h \sin u_i z \sin p_j (h-z) dz \right], \tag{27}$$

$$M_c[i,j] = \frac{2}{h} \left[\int_0^c \cos u_i z \cos q_j z dz + \alpha_j \int_c^h \cos u_i z \cos p_j (h-z) dz \right], \tag{28}$$

$$M_r[i,j] = \frac{2}{h} \int_0^c \cos u_i z \cos r_j z dz, \tag{29}$$

and a vector coefficient has also been defined whose elements are

$$L[i] = \frac{2}{h} \left[\int_0^c \cos u_i z \cosh kz dz + \cosh kc \int_c^h \cos u_i z dz \right]. \tag{30}$$

Evaluating the integrals leads to the results given in Ref. 2.

From $jm(23) - \mathbf{u}(24)$ and $b\Lambda_m(\mathbf{u}b)$ (23)–(25), we eliminate $\mathbf{C}_m^{(1)}$ to get a system of the form

$$\mathbf{A}_{11}\mathbf{C}_m^{(2)} + \mathbf{A}_{12}\mathbf{D}_m = \mathbf{K}_i \mathbf{C}_m^{(0)} + \mathbf{L}_1 C_{m0}^{(0)}, \tag{31}$$

$$\mathbf{A}_{21}\mathbf{C}_m^{(2)} + \mathbf{A}_{22}\mathbf{D}_m = \mathbf{K}_2 \mathbf{C}_m^{(0)} + \mathbf{L}_2 C_{m0}^{(0)}, \tag{32}$$

where the matrices $\mathbf{A}_{ij}$ and $\mathbf{K}_i$ $(i,j = 1,2)$ are

$$\mathbf{A}_{11} = Jm\mathbf{M}_s \mathbf{p} - \mathbf{u}\mathbf{M}_c, \tag{33}$$

$$\mathbf{A}_{12} = \mathbf{u}[b\mathbf{M}_r \mathbf{s} M_m(\mathbf{s}b) + \lambda \mathbf{L} \mathbf{R}_{m+1}^T], \tag{34}$$

$$\mathbf{A}_{21} = b[\mathbf{M}_s \Lambda_m(\mathbf{p}b) - \mathbf{M}_c M_m(\mathbf{p}b)]\mathbf{p}, \tag{35}$$

$$\mathbf{A}_{22} = -J[m\mathbf{M}_r - \lambda \mathbf{L} \mathbf{R}_{m+1}^T], \tag{36}$$

$$\mathbf{K}_1 = 0, \quad \mathbf{K}_2 = \mathbf{I}, \tag{37}$$

where $\mathbf{I}$ is the unity matrix. In addition, the following column vectors have been introduced,

$$\mathbf{L}_1 = Jm\lambda \mathbf{u}\mathbf{L}, \quad \mathbf{L}_2 = m\lambda \mathbf{L}. \tag{38}$$

The solution of Eqs. (31) and (32) found by inverting $\mathbf{A}_{21}$ is

$$\mathbf{D}_m = (\mathbf{A}_{12} - \mathbf{A}_{11}\mathbf{A}_{21}^{-1}\mathbf{A}_{22})^{-1}[(\mathbf{K}_1 - \mathbf{A}_{11}\mathbf{A}_{21}^{-1}\mathbf{K}_2)\mathbf{C}_m^{(0)} + (\mathbf{L}_1 - \mathbf{A}_{11}\mathbf{A}_{21}^{-1}\mathbf{L}_2)C_{m0}^{(0)}], \tag{39}$$

$$\mathbf{C}_m^{(2)} = -\mathbf{A}_{21}^{-1}(\mathbf{A}_{22}\mathbf{D}_m - \mathbf{K}_2 \mathbf{C}_m^{(0)} - \mathbf{L}_2 C_{m0}^{(0)}). \tag{40}$$

With $\mathbf{C}_m^{(2)}$ known, the coefficients vector $\mathbf{C}_m^{(1)}$ can be found from Eq. (23).

IV. POTENTIAL OF A FILAMENTARY CURRENT LOOP

A. Truncated region Green's function

The source coefficients can be identified from the explicit series solution for a coil in the nonconductive region between the truncation planes. The fields of an offset bobbin coil[7] and a rotary coil[8] have been derived previously for an unbounded domain using the fundamental solution $1/4\pi R$ for the Laplace problem. In keeping with a first-principles approach, we express the magnetic scalar potential representing the TE field in terms of the corresponding Green's function for the truncated region. This kernel is a solution of

$$\nabla^2 G^{(0)}(\mathbf{r}|\mathbf{r}) = -\delta(\mathbf{r}-\mathbf{r}), \tag{41}$$

satisfying the Neumann boundary condition $\partial G^{(0)}/\partial z=0$ at $z=0$ and $z=h$. The Green's function can be derived by adapting Dougall's method for the corresponding Dirichlet problem[9,10] to solve the Neumann problem. For the singular point on the axis of a cylindrical polar coordinate system, it has been shown that[11]

$$G^{(0)}(r,z,z') = -\frac{1}{2\pi h}\log r + \frac{1}{\pi h}\sum_{i=1}^{\infty}\cos u_i z \cos u_i z' K_0(u_i r), \tag{42}$$

where r is the radial distance from the singular point. As before, putting $u_i = i\pi/h$ ensures that the Neumann condition at $z=h$ is satisfied.

The coordinates can be transformed by using the addition theorem for the K_0 Bessel function,[10]

$$K_0(ur) = \sum_{m=-\infty}^{\infty} K_m(u\rho_>) I_m(u\rho_<) e^{Jm(\phi-\phi')}, \tag{43}$$

where $r^2=\rho^2+\rho'^2-2\rho\rho'\cos(\phi-\phi')$ and we write $\rho_>$ to denote the greater of ρ and ρ', while $\rho_<$ is the lesser. Correspondingly, the log function in Eq. (42) can be expressed as a series by applying the cosine rule factored with the cosine written in experimental form. Expanding the log of the factors using Taylor's series gives

$$\log r = \log \rho_> - \frac{1}{2}\sum_{m\neq 0}\frac{1}{|m|}\left(\frac{\rho_<}{\rho_>}\right)^{|m|} e^{Jm(\phi-\phi')}, \tag{44}$$

where the summation over m includes all positive and negative integers but excludes $m=0$. Combining Eqs. (43), (44), and (42) gives the required kernel

$$G^{(0)}(\mathbf{r}|\mathbf{r}') = -\frac{1}{2\pi h}\log \rho_> + \frac{1}{4\pi h}\sum_{m\neq 0}\frac{1}{|m|}\left(\frac{\rho_<}{\rho_>}\right)^{|m|} e^{Jm(\phi-\phi')} + \frac{1}{\pi h}\sum_{i=1}^{\infty}\cos u_i z \cos u_i z' \times \sum_{m=-\infty}^{\infty} K_m(u_i\rho_>) I_m(u_i\rho_<) e^{Jm(\phi-\phi')}, \tag{45}$$

which is the Neumann Green's kernel for a domain truncated by parallel planes.

B. Application of Green's second theorem

The field in the homogeneous domain is here represented by the magnetic scalar potential defined such that $\mathbf{B}=\nabla\psi$. The potential is a solution of

$$\nabla^2\psi = 0, \tag{46}$$

satisfying the same boundary conditions as Green's kernel, namely, $\partial\psi/\partial z=0$ at $z=0$ and $z=h$. To derive the coil field, we follow a procedure in which the potential due to a circular current filament is found first in a local coordinate system and then in global coordinates. Finally, the filament potential is integrated to get the corresponding potential for a coil of rectangular cross section.

According to a well-known equivalence principle,[12] the field of a filamentary current loop is the same as that of an infinitesimally thin magnetic shell at an arbitrary open surface bounded by the filament. We apply this principle to a circular loop taking the shell to be a circular disk. The magnetic shell is the physical representation of what is referred to in the theoretical interpretation of Green's second theorem as a double layer potential. The discontinuity/continuity conditions at the shell reflect the characteristics of such a potential, which are that the potential is discontinuous and the normal derivative of the potential is continuous. At the shell,

$$\psi_+ - \psi_- = -\mu_0 I, \qquad \left.\frac{\partial\psi}{\partial z}\right|_+ - \left.\frac{\partial\psi}{\partial z}\right|_- = 0, \tag{47}$$

where the $\pm$ subscripts denote the limiting values of the function as the shell is approached from the positive of negative direction of a particular coordinate. The first of these relationships shows that the magnetic scalar potential has a jump related to the magnetic dipole density which is constant over the shell surface.[13] The second reflects the fact that the normal component of the magnetic flux density is continuous at the shell.

By applying Green's second theorem to a surface enclosing the magnetic disk, using Eqs. (41) and (46) and then collapsing the closed surface onto the open surface of the disk, S_0, say, we get

$$\psi_\circ(\mathbf{r}) = -\mu_0 I\int_{S_\circ}\nabla' G^{(0)}(\mathbf{r}'|\mathbf{r})\cdot d\mathbf{S}', \tag{48}$$

where Eq. (47) has been used.

V. SOURCE COEFFICIENTS

A. Offset bobbin

The potential of a loop, radius ρ_0, whose axis is in the z direction is found from Eqs. (48) and (45). We use r and φ to denote local cylindrical coordinates whose axis passes through the center of the loop. Because the gradient in Eq. (48) is z directed in this case, terms independent of z in Eq. (45) are eliminated. The integral over φ eliminates all but the $m=0$ term to give the filament potential,

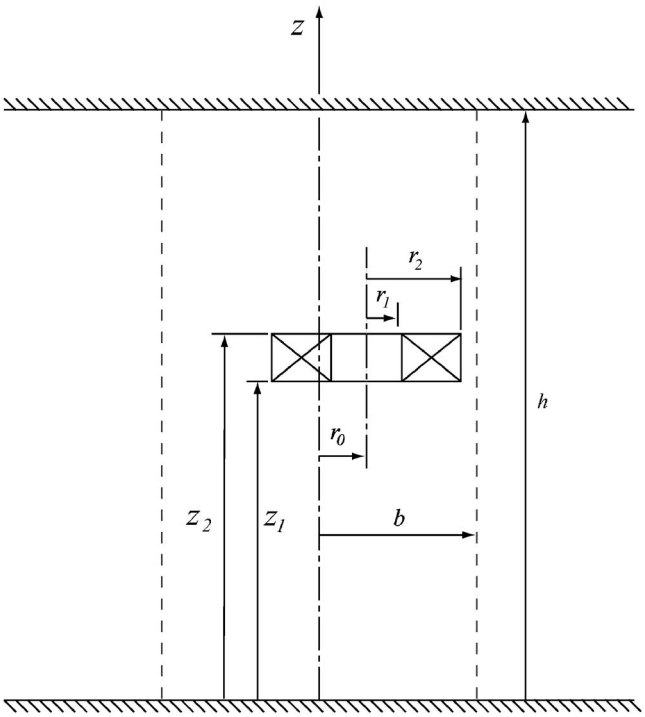

FIG. 3. Offset bobbin coil in a homogeneous nonconductive truncated domain. The source coefficients are identified from the explicit series expansion for the TE potential that describes the solution in this region.

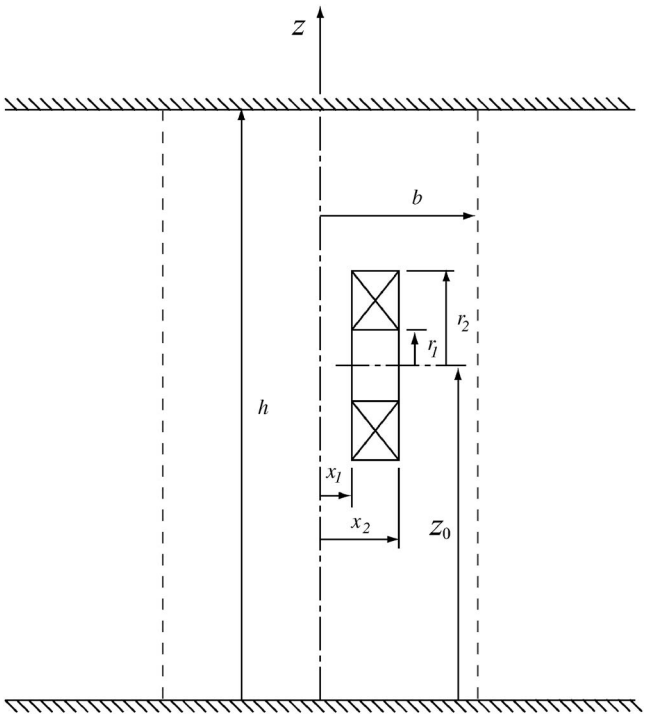

FIG. 4. A rotary coil in a homogeneous nonconductive truncated region. From the TE solution in this region, we identify the source expansion coefficients for the coil.

$$\psi_{\circ}(r,z) = \frac{2\mu_0 I}{h}\sum_{i=1}^{\infty} \cos u_i z \sin u_i z' K_0(u_i r) I_1(u_i \rho_0), \tag{49}$$

for $r > \rho_0$. Integrating over the rectangular cross section of a coil, whose turn density is ν and using the probe parameters shown in Fig. 3, we get the coils magnetic scalar potential,

$$\psi_c^{(0)}(r,z) = \frac{2\mu_0 \nu I}{h}\sum_{i=1}^{\infty} \cos u_i z K_0(u_i r) \times \frac{\cos u_i z_i - \cos u_i z_2}{u_i^3}\Phi(u_i r_2, u_i r_1), \tag{50}$$

in the region such that $r > r_2$, where

$$\Phi(a_2,a_1) = \int_{a_1}^{a_2} I_1(x) x dx. \tag{51}$$

Equation (50) gives the magnetic scalar potential of the offset coil in a local polar coordinate system whose axis coincides with that of the coil. The expression for the potential in the global coordinate system defined with reference to the borehole axis is found using the addition theorem (43),

$$\psi_m^{(0)}(\rho,z) = \frac{2\mu_0 \nu I}{h}\sum_{i=1}^{\infty} \cos u_i z K_m(u_i \rho) \times \frac{\cos u_i z_1 - \cos u_i z_2}{u_i^3}\Phi(u_i r_2, u_i r_1) I_m(u_i r_0), \tag{52}$$

for $\rho > r_0 + r_2$. Comparing Eq. (8) to Eq. (52), we deduce that

$$C_{mi}^{(0)} = \frac{2\mu_0 \nu I}{h}\left(\frac{\cos u_i z_1 - \cos u_i z_2}{u_i^3}\right) \times \Phi(u_i r_2, u_i r_1) K_m(u_i b) I_m(u_i r_0), \tag{53}$$

and that $C_{0i}^{(0)} = 0$. This defines the source coefficients for the offset bobbin coil.

B. Rotary coil

The source coefficients for the rotary coil (Fig. 4) are calculated following the procedure similar to that given previously for the unbounded domain problem.[8] However, the derivation of these coefficients for the truncated Neumann problem differs sufficiently in its details to warrant further explanation, especially with regard to the contribution from the zero order ($i=0$) Fourier series with respect to azimuthal dependence.

The zero order series for a coil can be derived from the corresponding zero order kernel [Eq. (44)], starting with the solution for a circular filament centered at a point on the z axis (Fig. 5). To separate the zero order term in keeping with the form of Eq. (45), we correspondingly decompose the loop solution,

$$\psi_{\circ} = \psi_0 + \sum_{i=1}^{\infty} \psi_i, \tag{54}$$

compute the leading term from

$$\psi_0 = -\mu_0 I \int_{S_0} \nabla' g^{(0)} \cdot d\mathbf{S}' \tag{55}$$

and the terms in the summation from

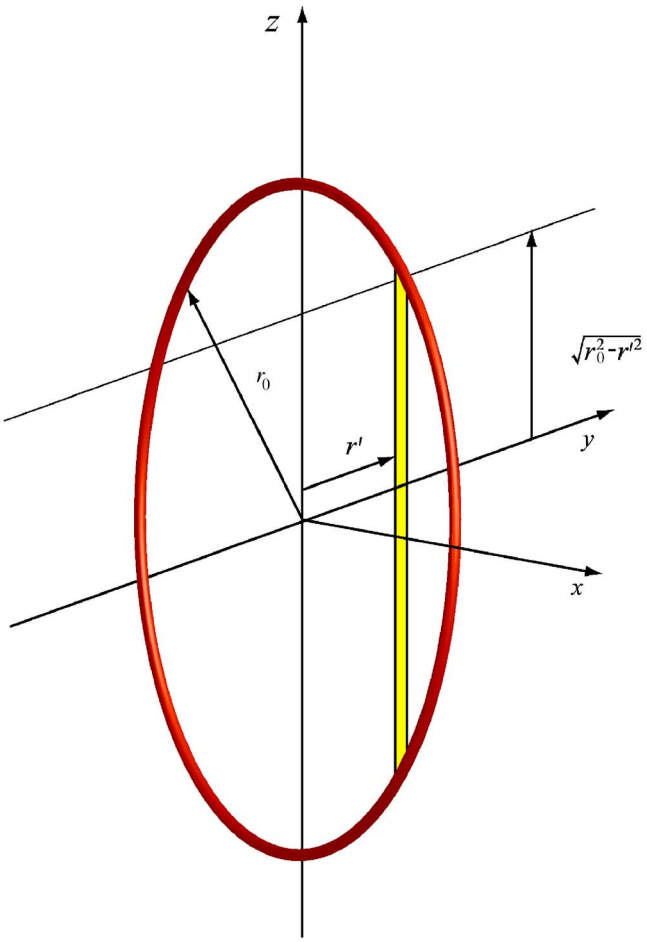

FIG. 5. (Color online) Filamentary loop with its axis in the x direction.

$$\psi_i = -\mu_0 I \int_{S_0} \nabla' G_i^{(0)} \cdot d\mathbf{S}', \tag{56}$$

where, using local coordinates (r, φ),

$$g^{(0)} = -\frac{1}{2\pi h} \log r_> + \frac{1}{4\pi h} \sum_{n\neq 0} \frac{1}{|n|} \left(\frac{r_<}{r_>}\right)^{|n|} e^{Jn(\varphi-\varphi')} \tag{57}$$

and

$$G_i^{(0)} = \frac{1}{\pi h} \cos u_i z \cos u_i z' \times \sum_{m=-\infty}^{\infty} K_m(u_i\rho_>) I_m(u_i\rho_<) e^{Jm(\phi-\phi')}. \tag{58}$$

The normal derivative in Eqs. (55) and (56) gives rise to a term $\pm(1/r')(\partial/\partial\varphi')e^{jm\varphi'}$, which has a constant value over half the circular area enclosed by the filament and a different value over the other half, depending on whether $\varphi = \pm\pi/2$. Adding these constants gives rise to a factor $(2n/r')\sin(n\pi/2)$.

Considering first the evaluation of Eq. (55), the surface integral can be reduced to an integral with respect to z and an integral with respect to r', but since the zero order kernel [Eq. (57)] is independent of z, the latter integral is trivial and simply gives rise to a factor of $2\sqrt{r_0^2-r'^2}$ as represented by the length of the elemental strip in Fig. 5. By integrating with respect to r', we get

$$\psi_0 = \sum_{n\neq 0} \frac{e^{Jn\varphi}}{r^{|n|}} c_{|n|}, \tag{59}$$

where

$$c_n = -\frac{\mu_0 I}{\pi h} a_n \sin(n\pi/2) r_0^{n+1}, \tag{60}$$

and the coefficients a_n arising from the radial integral are $a_1 = \pi/4$ with

$$a_n = \int_0^1 \xi^{|n|-1}\sqrt{1-\xi^2}\, d\xi = \frac{\pi}{2^{(n+3)/2}} \frac{1\cdot 3\cdot 5\cdots(n-2)}{\left(\frac{n+1}{2}\right)!}, \tag{61}$$

where $n = 3, 5, 7\ldots$.

We express $r^{|n|}e^{jn\varphi}$ in terms of a coordinate system in which the loop lies in the plane $x = x_0$ by writing

$$\eta = \zeta - x_0, \tag{62}$$

where $\eta = re^{j\varphi}$ and $\zeta = \rho e^{j\phi}$ are complex variables. Elementary analysis gives

$$\sum_{n=1}^{\infty} \frac{c_n}{\eta^n} = \sum_{n=1}^{\infty} \frac{c_n}{\zeta^n} \sum_{\ell=0}^{\infty} \frac{(n+\ell-1)!}{(n-1)!\ell!} \left(\frac{x_0}{\zeta}\right)^{\ell} = \sum_{m=1}^{\infty} \frac{1}{\zeta^m} \sum_{n=1}^{m} \frac{(m-1)!}{(m-n)!(n-1)!} x_0^{m-n} c_n. \tag{63}$$

In reordering the series above, we defined $m = n+\ell$ and noted that since ℓ is non-negative, n cannot exceed m, which dictates the upper limit of the inner sum. Transformation of Eq. (59) is achieved using Eq. (63) and its complex conjugate to take account of negative phase factors. Hence, the transformation of Eq. (59) to global coordinate yields

$$\psi_0 = \sum_{m\neq 0} \frac{e^{Jm\phi}}{\rho^{|m|}} \sum_{n=0}^{|m|} \frac{(|m|-1)!}{(|m|-n)!(n-1)!} x_0^{|m|-n} c_n. \tag{64}$$

Integrating over the coil cross section for a coil whose turn density is ν and identifying the zero order expansion coefficients with reference to Eq. (8) give

$$C_{m0}^{(0)} = -\frac{\mu_0 \nu I}{\pi h b^m} \sum_{n=1}^{|m|} \frac{a_n \sin\left(n\frac{\pi}{2}\right)(|m|-1)!}{(|m|-n+1)!(n-1)!} \times (x_2^{|m|-n+1} - x_1^{|m|-n+1}) \left(\frac{r_2^{n+2} - r_1^{n+2}}{n+2}\right). \tag{65}$$

To determine the remaining source coefficients for a rotary coil, we proceed by first using equation Eq. (58) together with Eq. (56) to give the contribution to the potential of a filamentary loop on the axis of a cylindrical polar coordinate system associated with the eigenvalue, u_i. This contribution has the form

$$\psi_i = \cos u_i z \sum_m K_m(u_i r) e^{-Jm\varphi} c_{mi}, \tag{66}$$

where

$$c_{mi} = -\frac{4\mu_0 \nu I}{\pi h} \frac{m}{u_i} \sin m\frac{\pi}{2} \cos u_i z_0 \times \int_0^{u_i r_0} \frac{1}{\xi} \sin\sqrt{u_i^2 r_0^2 - \xi^2} I_m(\xi) d\xi. \tag{67}$$

The change in the coordinate system can be accomplished using[14]

$$K_m(u_i r) e^{-Jm\varphi} = \sum_\ell K_\ell(u_i \rho) I_{\ell-m}(u_i x_0) e^{-J\ell\phi}. \tag{68}$$

Integrating over x_0 and r_0 and comparing the resulting expression for the magnetic scalar potential with the general form [Eq. (53)] show that

$$C_{mi}^{(0)} = -\frac{4\mu_0 \nu I}{\pi h} \cos u_i z_0 \frac{m}{u_i^3} \sin m\frac{\pi}{2} K_m(u_i b) \times \sum_{n=-\infty}^{\infty} \Psi_{m-n}(u_i x_2, u_i x_1) \Xi_n(u_i r_2, u_i r_1), \tag{69}$$

where

$$\Psi_m(\alpha_2, \alpha_1) = \int_{\alpha_1}^{\alpha_2} I_m(x) dx \tag{70}$$

and

$$\Xi_n(v_2, v_1) = \int_{v_1}^{v_2} \int_0^v \frac{1}{\xi} I_n(\xi) \sin(\sqrt{u^2 - \xi^2}) d\xi dv. \tag{71}$$

This completes the determination of the source coefficients for the rotary coil.

VI. IMPEDANCE CHANGE

It has been shown using a reciprocity theorem that the coil impedance change due to induced current is given by an integral over a surface enclosing the coil.[7] Taking the surface to be a cylinder with radius b and expressing the integrand in terms of magnetic scalar potentials give

$$\Delta Z = -\frac{j\omega}{\mu_0 I^2} \int_0^h \int_{-\pi}^{\pi} \left[\psi^{(1)} \frac{\partial \psi^{(0)}}{\partial \rho} - \psi^{(0)} \frac{\partial \psi^{(1)}}{\partial \rho} \right]_{\rho=b} b d\varphi dz. \tag{72}$$

By substituting for $\psi^{(0)}$ and $\psi^{(1)}$ and using the Wronskian

$$I_m'(z) K_m(z) - I_m(z) K_m'(z) = \frac{1}{z}, \tag{73}$$

we get the general expression for the impedance change of a coil in a borehole and a truncated domain,

$$\Delta Z = -\frac{j\omega}{\mu_0 I^2} \pi h \left[\sum_m^{\infty} m C_{m0}^{(0)} C_{m0}^{(1)} + \sum_{i=1}^{\infty} \frac{C_{mi}^{(0)} C_{mi}^{(1)}}{I_m(u_i b) K_m(u_i b)} \right], \tag{74}$$

where $C_{m0}^{(0)}$ is zero for the offset bobbin and is given by Eq. (65) for the rotary coil, $C_{mi}^{(0)}$ is given by Eq. (53) for the offset bobbin and Eq. (69) for the rotary coil, $C_{m0}^{(1)}$ is given by Eq. (19), and $C_{mi}^{(1)}$ is determined from Eq. (23) via Eqs. (40) and (39).

TABLE I. Coil and borehole parameters. The offset of the bobbin coil is r_0 (Fig. 6), and the distance of the rotary coil base from the axis is x_1 in mm (Fig. 4). $\ell = x_2 - x_1$ is the axial length of the coil.

Coil	Borehole	
r_1	6.95 mm σ	24.36 MS/m
r_2	9.35 mm μ_r	1
ℓ	6.70 mm b	20 mm
N	335	
r_0	4.1 mm	
x_1	5.63 mm	

VII. RESULTS

The results for a bobbin coil with zero offset ($d=0$) are a special case of an axisymmetric geometry. In this case, the model is simplified since $I_m(\mathbf{u}d)=0$ and, hence, every term in which $m \neq 0$ vanishes. Predictions for axisymmetric solution without edge effects compare well with experimental data[15] but here, we will present some numerical results for the same offset bobbin coil and test-piece data used in the infinite borehole case.

Calculations were carried out using MATHEMATICA to compute the impedance change of the coil near the borehole edge. Significant considerations in relation to accuracy are the choice of the truncated domain size h and the number of terms in the m and i summations, namely, N_m and N_i. Reference to the case of the infinite length borehole was very helpful in this respect.

Theoretical results from the truncated domain series expressions were compared to results from the exact expressions in Ref. 8, and it was observed that (as a rule of thumb) for $h=nr_2$ and $N_i=2n$ with $n=20$, we obtained an agreement of the order of 1% for all frequencies. This means that the

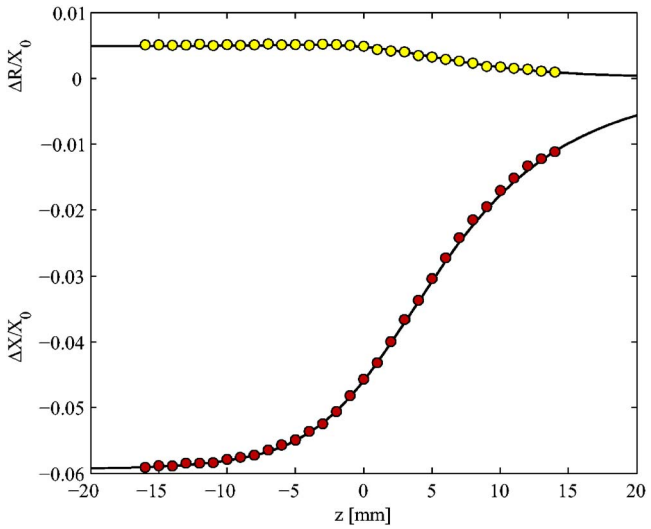

FIG. 6. (Color online) Variation of coil impedance change of an offset bobbin coil as it traverses the borehole edge. Measurements were made at an excitation frequency of 10 kHz.

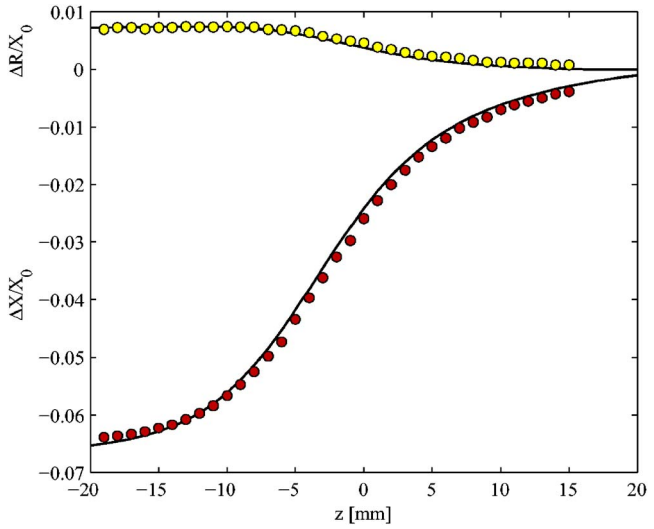

FIG. 7. (Color online) Variation of coil impedance change of a rotary coil as a function of axial position. The measurement were made at an excitation frequency of 10 kHz.

square matrices were 40×40. The chosen value for h ensures that the coil center is about ten outer coil radii away from the outer boundaries and, thus, the truncated geometry simulates the infinite domain adequately.

The theoretical results (calculated using the parameters in Table I) for the infinite borehole were compared to frequency scans with the coil located far from the borehole edge in order to assess the degree of agreement with experiment and whether any liftoff adjustment was required.[16] No such distance correction between the coil and borehole wall was necessary; therefore, there are no free parameters in the calculations. Then, the same coil, whose self-inductance is 1.754 mH (1.752 mH according to theory), was scanned across the borehole edge in the two orientations described, (a) offset and (b) rotary. Figure 6 shows the variation of the impedance change of an offset bobbin coil as a function of axial position measured with respect to the edge of the hole. Impedance variations for a rotary coil as a function of position are shown in Fig. 7. The predictions are compared with experimental measurements and again show good agreement.

VIII. CONCLUSION

Closed-form expressions for the impedance of a cylindrical coil and for the electromagnetic field have been derived for an eddy current probe coil located near the edge of a deep borehole. Using transverse electric and transverse magnetic scalar potentials to represent the electromagnetic field in an axially truncated region, the potentials are expressed in terms of series expansions. The expansion coefficients have been found by mode matching across the boundary of the extended hole. Comparison of coil impedance predictions agrees well with experimental measurements, the calculations take only a few seconds and the errors are easily controlled by adjusting the number of terms in the series and the location of the truncation boundaries.

The approach can be extended to deal with a through hole in a plate whose thickness is of the order of the coil dimensions or less. Because eddy current inspection of the borehole structure is common, it is of interest to develop an inspection model that takes account of the presence of a crack at the edge of the hole. This may be done at low computational cost by using Green's kernel for the structure with a singular source in the metal. This can be accomplished by using the approach described in this article.

ACKNOWLEDGMENTS

The authors would like to thank Rob Ditchburn of DSTO Melbourne for conducting the experiments. This material is based on the work supported by the Air Force Research Laboratory under Contract No. FA8650-04-C-5228 at Iowa State University's Center for NDE.

[1] C. V. Dodd and W. E. Deeds, J. Appl. Phys. **39**, 2829 (1968).
[2] T. P. Theodoulidis and J. R. Bowler, Proc. R. Soc. London, Ser. A **461**, 3123 (2005).
[3] T. P. Theodoulidis, Int. J. Appl. Electromagn. Mech. **19**, 207 (2004).
[4] T. P. Theodoulidis, J. Appl. Phys. **93**, 3071 (2003).
[5] J. R. Bowler and T. P. Theodoulidis, J. Phys. D **38**, 2861 (2005).
[6] M. Abramowitz and I. Stegun, *Handbook of Mathematical Fuctions with Formulas, Graphs, and Mathematical Tables* (Dover, New York, 1972).
[7] T. P. Theodoulidis, Res. Nondestruct. Eval. **14**, 111 (2002).
[8] S. K. Burke and T. P. Theodoulidis, J. Phys. D **37**, 485 (2004).
[9] J. Dougall, Proc. Edinb. Math. Soc. **18**, 33 (1900).
[10] A. Gray and G. B. Mathews, *A Treatise on Bessel Functions and Their Applications* (Dover, New York, 1966).
[11] S. Murashima, Jpn. J. Appl. Phys. **12**, 1232 (1973).
[12] J. A. Stratton, *Electromagnetic Theory* (McGraw-Hill, New York, 1941).
[13] To show that the magnetic shell has a constant magnetic dipole density, use Stokes theorem applied to the integral of the magnetic field along a path enclosing the filament.
[14] G. N. Watson, *Treatise on the Theory of Bessel Functions*, 2nd ed. (Cambridge University Press, Cambridge, 1944).
[15] S. K. Burke, J. R. Bowler, and T. P. Theodoulidis, *Review of Progress Quantitative Nondestructive Evaluation*, edited by D. O. Thompson and D. Chimenti (AIP, Melville, NY, 2006), Vol. 25, pp. 361–368.
[16] T. P. Theodoulidis and J. R. Bowler, *Review of Progress Quantitative Nondestructive Evaluation*, edited by D. O. Thompson and D. Chimenti (AIP, Melville, NY, 2007), Vol. 26, pp. 233–240.